**IOP** Publishing European Journal of Physics

Eur. J. Phys. **38** (2017) 045804 (18pp) https://doi.org/10.1088/1361-6404/aa7147

# Sound and vision: visualization of music with a soap film

**C Gaulon[1], C Derec[1], T Combriat[2], P Marmottant[2] and F Elias[1,3]**

[1] Laboratoire Matière et Systèmes Complexes UMR 7057, Université Paris Diderot, Sorbonne Paris Cité, CNRS, F-75205 Paris, France

[2] Laboratoire Interdisciplinaire de Physique LIPhy, Université Grenoble Alpes and CNRS UMR 5588, F-38402 Saint Martin d'Hères, France

[3] Sorbonne Universités, UPMC Univ Paris 06, 4 place Jussieu, F-75252 Paris cedex 05, France

E-mail: florence.elias@univ-paris-diderot.fr

Received 9 February 2017, revised 11 April 2017
Accepted for publication 5 May 2017
Published 9 June 2017

**Abstract**

A vertical soap film, freely suspended at the end of a tube, is vibrated by a sound wave that propagates in the tube. If the sound wave is a piece of music, the soap film 'comes alive': colours, due to iridescences in the soap film, swirl, split and merge in time with the music (see the snapshots in figure 1 below). In this article, we analyse the rich physics behind these fascinating dynamical patterns: it combines the acoustic propagation in a tube, the light interferences, and the static and dynamic properties of soap films. The interaction between the acoustic wave and the liquid membrane results in capillary waves on the soap film, as well as non-linear effects leading to a non-oscillatory flow of liquid in the plane of the film, which induces several spectacular effects: generation of vortices, diphasic dynamical patterns inside the film, and swelling of the soap film under certain conditions. Each of these effects is associated with a characteristic time scale, which interacts with the characteristic time of the music play. This article shows the richness of those characteristic times that lead to dynamical patterns. Through its artistic interest, the experiments presented in this article provide a tool for popularizing and demonstrating science in the classroom or to a broader audience.

Keywords: soap films, acoustic resonances, light interferences, acoustofluidics

(Some figures may appear in colour only in the online journal)

 © 2017 European Physical Society Printed in the UK 

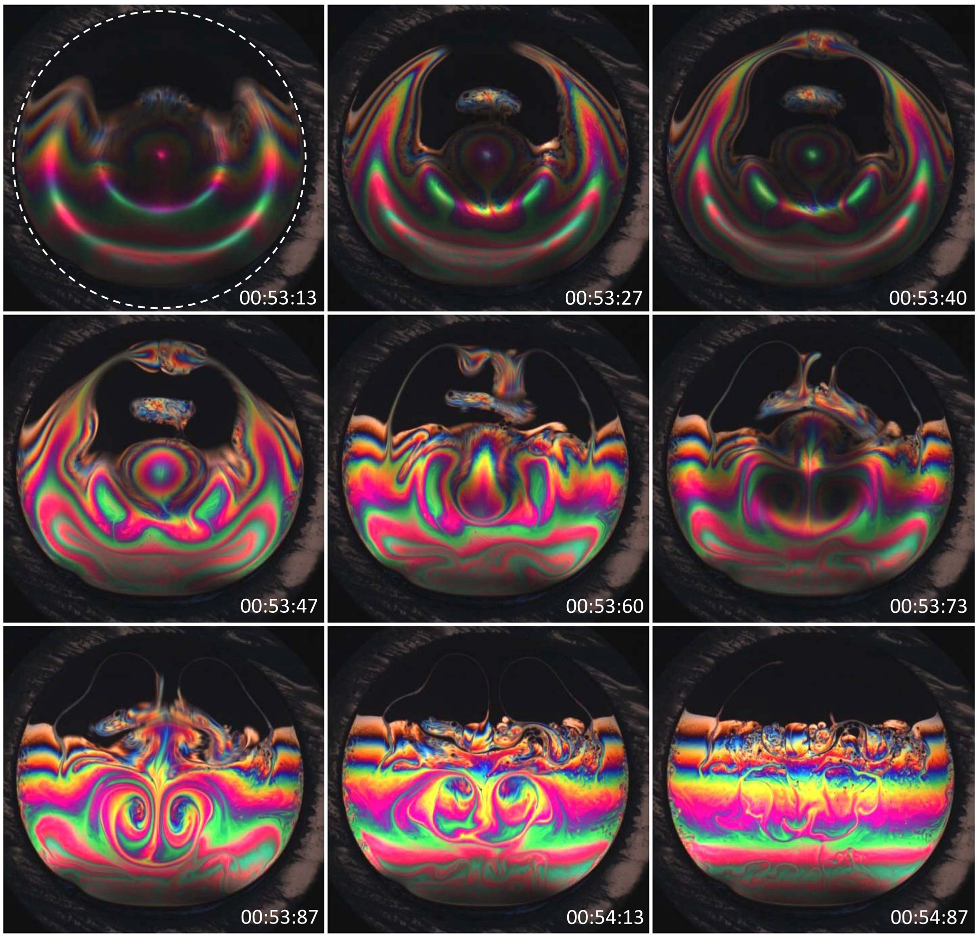


**Figure 1.** Snapshots of the observed dynamics in a freely suspended vertical soap film submitted to an acoustic wave and illuminated by a white light. The dashed white circle on the first picture shows the internal border of the tube (of diameter $D = 26$ mm) delimiting the soap film. Piece of music: *Lucilla*, from the album 'Aeroplanando', by Choro de Rua (2013) (see the video at the following link: https://youtu.be/ch1m9vrgAzM). The time of each snapshot is indicated in the format minute:seconds: hundredths of second, starting from the beginning of the piece.

## 1. Introduction

For many centuries, both scientists and artists have been searching for connections between sound and vision, in other words between what we hear and what we see. Historically, these connections were first sought between music and colour. Aristotle, in his *De sensu et sensibilibus*, considered seven colours distributed from black to white [1]. This was based on the analogy with the Pythagorean intervals in music that define seven notes: Aristotle transferred the consonances of tonal intervals to colours. Inspired by the work of the ancient Greeks, Newton represented the decomposition of white light through a prism with seven colours. In his *Opticks*, in 1704, this was illustrated with the so-called Newton circle, which shows the colours correlated with the musical notes A to G [2], as represented in figure 2(a). The

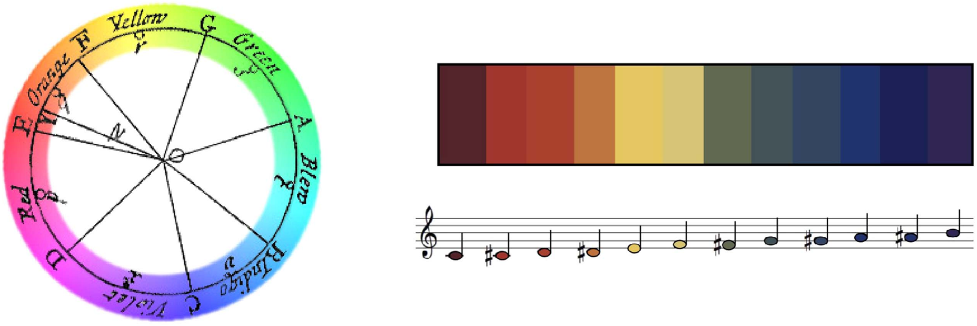


(a) (b)

**Figure 2.** Two different ways of associating colours to musical notes. (a) Newton's circle. Colours from red to violet are divided by notes, starting arbitrarily at D with purple colour (reproduced from [2]). (b) Rimington's chromatic scale in music and colour, starting arbitrarily at C with a dark red colour (inspired from [3]).

spectral colours are divided by the musical notes, the note D being arbitrarily placed between the red and the violet: the circle thus completes a full octave. In 1893, the british painter Alexander Wallace Rimington invented an instrument, also based on the correlation between colour and music, the Colour Organ [3]. A coloured light was projected when the associated note was played. In 2015, the National Gallery in London presented the exhibition 'Soundscapes', judiciously subtitled 'Hear the painting. See the sound' [4]. Some musicians and sound artists were asked to choose a painting from the museum collection, and compose a new piece of music in response, in order to create an immersive and original experience. Recently, the musician Nigel Stanford published a music-clip where the music is visualized using physics experiments [5], including Faraday instabilities, the use of ferrofluids, and the sand patterns of Chladni plates.

In this article, we propose a new way to visualize music, using a soap film. Similarly to Stanford's performances, the genuine connection between sound and vision comes from the fact that what we see (the transverse vibration of the soap film, the vortices) is generated by what we hear. Videos can bee seen in the indicated links.

On top of their artistic interest, soap films are commonly used to demonstrate science in the classroom or to a broader audience [6–9]. Soap films and bubbles consist of thin liquid films, which are stabilized by surfactant molecules; they tend to decrease their interfacial energy by minimizing the area of their interfaces. Hence, the science of soap films is by essence at a crossroads between physics, mathematics and chemistry. Soap films and bubbles also provide analogies with other physical systems, such as atmospheric phenomena (stratification and turbulence [10, 11]) and mathematics (catastrophe theory and minimisation problems [8, 9]).

Vibrating soap films and the associated patterns have fascinated physicists for a long time. In 1877, E B Tylor reported on the 'singular clearness and beauty' of the patterns formed on a soap film 'by talking, singing and playing a cornet in its neighborhood' [12]. One year later, S Taylor published drawings illustrating the symmetry of the patterns obtained when a horizontal soap film was submitted to a monochromatic acoustic wave [13]. Many studies have attempted to rationalize these phenomena [10, 14–18]. The underlying physics resides in the hydrodynamics of the liquid and the surrounding air, and the way those flows are coupled at the liquid interfaces of the thin film.

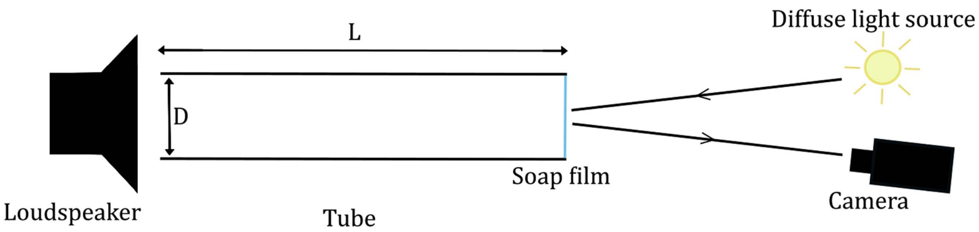


**Figure 3.** Sketch of the experimental set-up. The diffusive light source is obtained using a table lamp and a diffusive screen made of tracing paper between the lamp and the soap film.

In a previous article, soap films were used to visualize a monochromatic standing sound wave in a tube [19]. This visualization was based on the interaction between the soap films placed inside the tube, the acoustic wave and the optical wave. In the present article, only one film is formed at the end of a tube. The dynamics of the soap film is observed in response to a non-continuous acoustic forcing: music, applied at the other end of the tube. We analyse the physical phenomona involved in this rich and spectacular dynamics. This means that this experiment is an appropriate tool to teach the physics of light interference and acoustic resonance, as well as the vibrations of membranes and the physics of thin liquid films.

The article is organized as follows. In section 2, the set-up is described and some background is given: acoustic resonances in the tube, colours on the film due to interferences of the light, statics and dynamics of the liquid soap film. The dynamics of the soap film due to the acoustic forcing is then described in section 3, and illustrated in figure 1. The acoustic forcing generates transverse *capillary standing waves* on the liquid membrane (section 3.1). At large enough forcing amplitude, local thickness variation appears within the film: this thickness modulation is known as a *self-adaptation* mechanism (section 3.2). At larger forcing amplitudes, counter-rotative vortices appear within the soap film (section 3.3). The tangential flows inside the film eventually advect regions of different thicknesses, which do not mix and form two-dimensional drops in the film (section 3.4). A large recirculation of liquid inside the film has also been observed, which can lead to the *swelling* of a previously drained film (section 3.5). As a conclusion, we point out in section 4 the key elements to perform this sound and vision experiment in an aesthetic way.

## 2. Experimental set-up and scientific background

### *2.1. Experimental setup*

An acoustic wave is generated by a loudspeaker connected to a frequency generator. The loudspeaker is placed at one end of a horizontal cylindrical plexiglas tube, of length $L = 35.5$ cm, and internal diameter $D = 26$ mm. The tube is filled with air at ambient temperature and atmospheric pressure. At the other end of the tube, a vertical soap film is formed by placing the tube vertically and dipping its end into a soap solution, and by placing the tube back into the horizontal position. The soap solution is made of distilled water, 10% commercial washing liquid (Fairy® liquid, Dreft® or Dawn®—which are different brands of the same product by Procter and Gamble) and 10% glycerol (the percentages are indicated in volume). For the visualization of the soap film we use a diffuse light source, and a camera that receives the light reflected by the film (figure 3). The videos are recorded at a frame rate

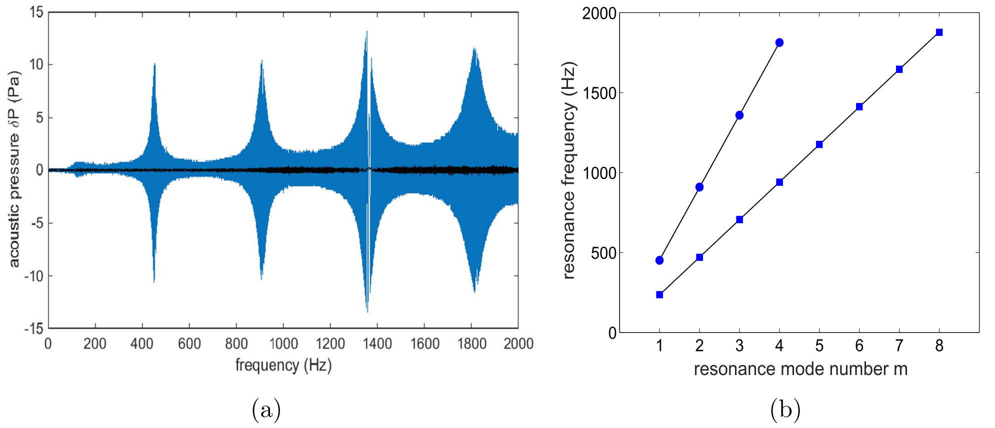


**Figure 4.** (a) Acoustic pressure $P$ versus the frequency $f$ of the forcing sound wave, measured at the end of the tube (blue curve) and at the same position without the tube (black curve). (b) Resonance frequencies versus the mode number $m$, for two different tube lengths: $L = 35.5$ cm (circles) and $L = 70$ cm (squares), of the same diameter $D = 26$ mm. The black lines correspond to the theoretical expression of the resonance frequencies, given by equation (1), and adjusting the end correction $C$ to the best fit.

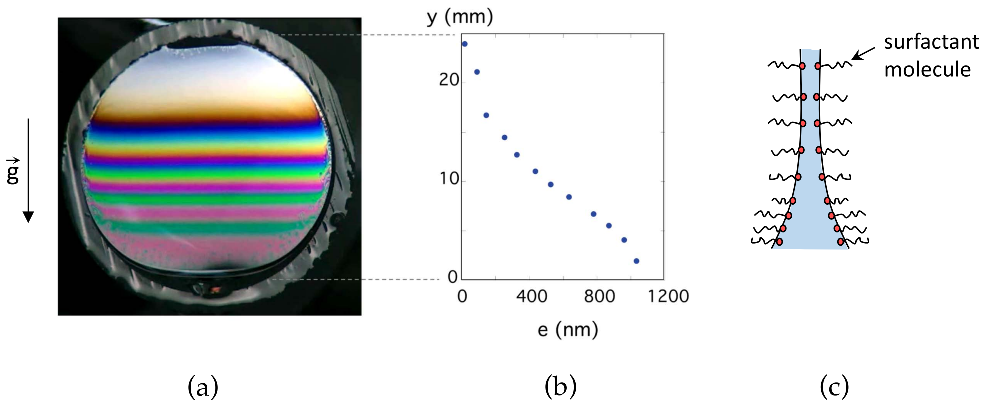


**Figure 5.** (a) Photograph of a soap film without any acoustic forcing: the soap film is vertical and displays a variation of colours, corresponding to the thickness gradient due to the gravitationally driven drainage. (b) Thickness of the film along the vertical direction $y$. The measurements are based on the colour of the film at height $y$. (c) Sketch of a cross-section of a vertical soap film: the thickness gradient is accompanied by a gradient of surface concentration of the surfactant molecules at the interfaces (not drawn to scale).

of approximately 13 frames per second. A video presenting the setup is available at the following link: https://youtu.be/wMFrfWZpVMM.

### *2.2. Acoustic resonances in a tube*

The cylindrical tube acts as a waveguide for the acoustic wave. Moreover, the acoustic pressure $P$ in the tube is maximum for a discrete number of frequencies, the resonance frequencies, as shown in figure 4. In the case of an open tube of length $L$, the resonance frequencies are given by [20]:

$$f_m = m\frac{v}{2(L + 2C)} \tag{1}$$

where $m$ is the resonance mode number and $v$ the sound velocity in air. $C$ represents the end correction (at each end), and is proportional to the diameter. The resonance frequencies $f_m$ are measured in figure 4(b) for two tubes of different lengths but of the same diameter, and plotted versus the resonance mode number $m$. The measurements are compared to equation (1) in figure 4(b), adjusting $C$, for each tube, to the best fit (taking $v = 343$ m s$^{-1}$). We obtain $C = (0.47 \pm 0.02)D$ for $L = 35.5$ cm and $C = (0.42 \pm 0.02)D$ for $L = 70$ cm: both cases are consistent with values found in the literature (see for example the theoretical model [21] where $C \simeq 0.42D$).

### *2.3. The physics of a soap film*

*2.3.1. Colours: light interferences.* At one end of the tube, a vertical soap film is freely suspended at the internal border of the tube. The film is illuminated with a white light source, and observed under the incidence angle using a video camera (see figure 3). A colourful pattern is visible on the soap film even when no acoustic forcing is imposed, as can be seen in figure 5(a): horizontal iridescent fringes are observed, which slowly move downwards in time.

These colours result from the interferences of the light reflected by both liquid–air interfaces, when the film thickness is of the order of the wavelength of light, as described in many references [8, 19]. Under a monochromatic illumination of wavelength $\lambda$, the intensity of the light reflected by the soap film would oscillate between zero and a maximum value, depending on the optical path difference $\delta$ between the light reflected by both interfaces of the film, with a periodicity of $\lambda$. The white light illumination contains all the wavelengths in the visible spectrum. Hence, the patterns corresponding to each wavelength add up incoherently, the total reflected intensity being modulated by the optical spectrum of the light source. As a result, the soap film appears white for $\delta \simeq 400$ nm, and then successively yellow, pink, blue, etc., when $\delta$ increases, which corresponds to a destructive interference for the complementary colors. When the optical path becomes larger than the coherence length of the light source (typically 1 $\mu$m for an incandescent light bulb), the iridescent pattern completely loses contrast and becomes uniformly white. In contrast, when $\delta$ is smaller than the visible wavelength (typically when $\delta < 200$ nm), the interferences are destructive and the soap films appears black. The colored interference fringes are referred to as Newton's shades, since Newton was the first to describe these shades in his *Opticks* [2].

The optical path $\delta$ depends on the thickness of a soap film, which can therefore be determined using charts that have been established using white light illumination [8, 22]. However, since the colors travel periodically through the entire visible spectrum when the thickness increases, the chart can be used only if the soap film thickness varies continuously and monotonously, starting from the black film, visible on the image. The soap film profile in figure 5 has been measured according to this method (with the area of black film visible at the top of the film).

*2.3.2. Statics and dynamics of a soap film.* Contrary to the case of a film made of pure water, a soap film can be stable in time. This stability is due to the surfactant molecules, which adsorb at the water-air interfaces, providing a repulsive interaction between the interfaces, which couterbalances the van der Waals attraction [23]. The competition between attractive and repulsive interactions results in an equilibrium thickness, of the order of a few tens of nanometers. Equilibrium soap films are referred to as black films: they indeed appear black when illuminated, because the optical path is smaller than the wavelength of the visible light.

However, soap films do not immediately reach their equilibrium thickness. A few seconds after their formation, vertical soap films display a pattern of parallel horizontal colorful fringes as shown in figure 5(a). The thickness stratification suggests that a hydrostatic equilibrium has been reached at short times, as described in many publications and summarized by Couder *et al* [10]. We recall here the points that are specifically relevant for describing the soap film behaviour in our experiment. In a vertical soap film, the surfactant concentration is larger at the bottom than at the top of the film, as sketched in figure 5(c): hence, a vertical gradient of surface tension $\gamma$ opposes the hydrostatic pressure exerted by the inner fluid:

$$2\frac{\mathrm{d}\gamma}{\mathrm{d}y} = \rho g\, e(y) \tag{2}$$

where $y$ is the vertical coordinate, $\rho$ the density of the liquid and $g$ the gravity acceleration. The prefactor 2 is due to the presence of two interfaces on the soap film. In the case of an insoluble surfactant, the equilibrium profile of the soap film can be predicted [10, 24]. However, this prediction is not valid in the case of a soluble surfactant, which corresponds to the majority of the experiments, since the use of soluble surfactants at high concentrations (i.e. larger that the critical micellar concentration) considerably increases the soap film stability [25].

Considering the 2D system formed by the surfactant molecules in interaction within one interface, the Marangoni force, caused by the gradient of surface tension, can be seen as an elastic restoring force, which counterbalances the 2D compression (or dilatation) of the surfactant molecules. Hence, the surfactant monolayer is actually provided with 2D visco-elastic properties. The surface elastic modulus of the soap film is defined as:

$$E = 2\,\frac{\mathrm{d}\gamma}{\mathrm{d}(\ln S)} = 2S\,\frac{\mathrm{d}\gamma}{\mathrm{d}S} = -2e\,\frac{\mathrm{d}\gamma}{\mathrm{d}e} \tag{3}$$

where $S$ is the surface of the film. The last term in equation (3) is obtained considering that the fluid is incompressible (constant volume $V = S \times e$).

Using equations (2) and (3), the surface elasticity can be estimated from the soap film profile [10]:

$$E = -\rho g e^2\,\frac{\mathrm{d}y}{\mathrm{d}e}. \tag{4}$$

In our experimental conditions (figure 5), $e \sim 1\ \mu$m and $\mathrm{d}y/\mathrm{d}e \sim -1,\ 5.10^4$, which leads to $E \sim 0.15$ mN m$^{-1}$.

On a timescale longer than a few seconds, the liquid flows down under its own weight and the thickness of the soap film decreases. This is revealed by the slow downwards motion of the coloured fringes. The interfaces covered with surfactant molecules are provided not only with 2D elastic properties but also with 2D viscous properties, hence the motion of the liquid inside the film is slowed down by the viscous friction against the interfaces. The velocity profile of the liquid between the interfaces is a Poiseuille profile with a non-zero velocity at the interfaces which are also set into motion (see [24, 26] for details). The drainage stops when the soap film has reached its equilibrium thickness.

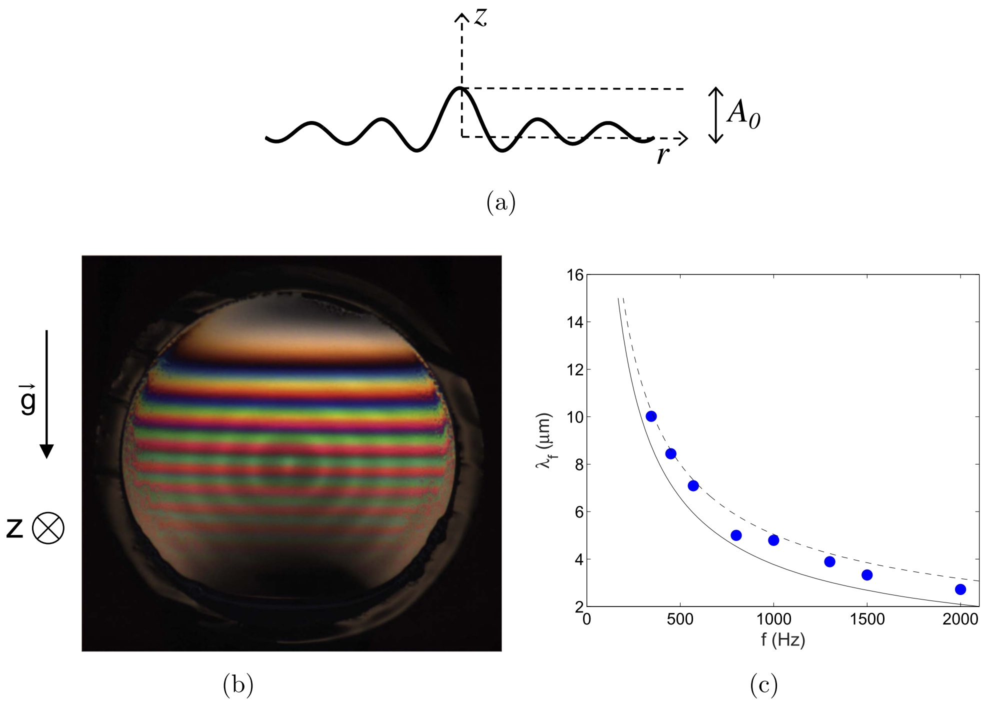


**Figure 6.** (a) Schematized side view of a vibrating film following a Bessel profile: $z(r) = A_0 J_0(2\pi r/\lambda_f)$. (b) Photograph (front view) of a vibrating soap film, presenting a standing capillary wave, visible via the bright concentric rings. The acoustic frequency is 860 Hz. (c) Wavelength $\lambda_f$ of the capillary waves as a function of the frequency $f$. The symbols represent the experimental points, and the black curves the theoretical dispersion relation given by equation (5), for two values of the thickness $e$ (full line: $e = 2\ \mu$m, dashed line $e = 0\ \mu$m).

## 3. Coupling sound and vision: 'seeing' the sound on a soap film

In this section, the elements that have been separately analyzed in the previous section are coupled, to describe the sound and vision experiment. Depending on the acoustic excitation, different phenomena appear. Capillary waves can be observed on the soap film even at small forcing amplitude. At larger amplitude the thickness profile is perturbed by the vibration according to a process called self-adaptation. When increasing the forcing amplitude, further non-linear effects appear. Amongst them, we describe the appearance of counter-rotative vortices.

### *3.1. Capillary waves*

Under acoustic forcing, the vibration of the air in the tube forces the soap film to move transversally: a transverse vibration wave propagates along the liquid membrane. The wave is reflected at the boundaries of the film and at its center. Due to the axial symmetry of the problem, this leads to the appearance of a circular standing wave on the soap film. This wave is characterized by the displacement $z(r, t) = A_0 J_0(2\pi r/\lambda_f)\cos(2\pi ft)$, where $z(r, t)$ is the transverse displacement from the equilibrium position at time $t$ and distance $r$ from the center of the film, $A_0$ is the amplitude at the center, $\lambda_f$ is the wavelength and $J_0$ the Bessel function of

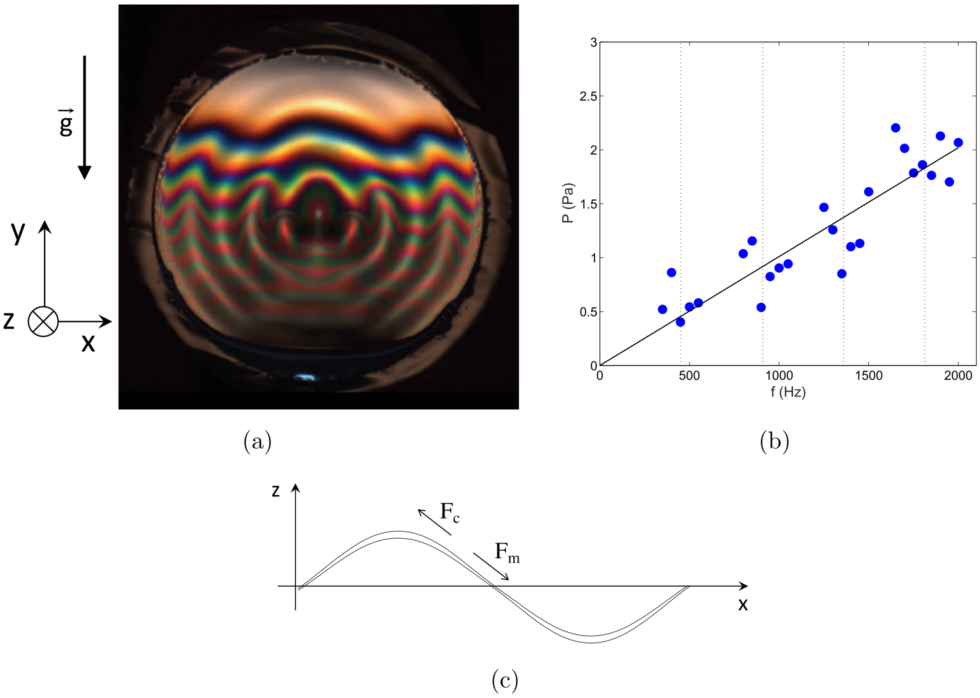


**Figure 7.** (a) Photograph of a soap film acoustically excited, showing self-adaptation. (b) Minimum amplitude of the pressure for the appearance of self-adaptation, as a function of the applied frequency. The measurements have been made around the resonance frequencies of the tube (indicated by the vertical dashed lines), where sufficiently high forcing amplitudes can be obtained. The black curve is a linear fit of the experimental points: $P = 1 \times 10^{-3} \times f$. Each measurement has been performed on a different soap film, by gradually increasing the amplitude of a monochromatic forcing until self-adaptation appears. (c) Sketch of a vibrating soap film exhibiting self-adaptation. The centrifugal force $F_c$ creates a tangential flow inside the film towards the antinodes, whereas the Marangoni force $F_m$ tends to homogenize the thickness of the film.

the first kind and zero order, whose profile is sketched in figure 6(a). When the soap film is illuminated and observed within a direction close to the normal incidence, the curved interface of the oscillating film acts as a curved mirror that focalizes the light reflected around the antinodes (caustics). This explains the appearance of bright rings on the soap film as shown in figure 6(b), whose number increases when the acoustic frequency increases[4]. This ring pattern allows the measurement, using image analysis, of the wavelength $\lambda_f$. The variation of $\lambda_f$ with the acoustic frequency can then be compared with previous works ([14, 15, 18] and references therein) that predict the following dispersion relation between the wavelength and the frequency, for a horizontal infinite soap film, and in the linear limit with $A_0$, $e \ll \lambda_f$:

[4] Note that a parallel illuminating beam light would generate a more contrasted ring pattern [27].

$$\lambda_f f = \sqrt{\frac{2\gamma}{\rho e + \rho_a \lambda_f/\pi}} \tag{5}$$

where $\rho$ and $\rho_a$ are respectively the densities of the soap solution and of the air. The wave propagation is characterized by the interplay between the surface tension $\gamma$ as the restoring force, and the inertia of the system. Note that the inertia of the air above and below the film on a typical distance $\lambda_f$ has to be taken into account, since $\rho_a \lambda_f$ and $\rho e$ are of the same order of magnitude.

Considering that in our experiments the thickness of the soap film is not homogeneous because of the gravitational drainage, we find a good agreement between the theoretical predictions and our measurements of $\lambda_f$, as shown in figure 6(c).

### *3.2. Self-adaptation of the thickness*

When increasing the amplitude of the acoustic excitation, the interference fringes are not horizontal anymore as shown in figure 7(a): they undulate and exhibit peaks around the antinodes of the transverse vibration. This means that a liquid flow has occured in the plane of the film, leading to a spatial modulation of the soap film thickness: the film is thinner around the vibration nodes and thicker around the antinodes. This phenomenon, already observed in a previous work (see [17]), is referred to as *self-adaptation*.

We have observed that the self-adaptation appears above a threshold value of the amplitude of the acoustic wave, which depends linearly on the frequency, as presented on figure 7(b). We develop here a simple argument to explain this effect, based on the modeling performed by Boudaoud *et al* [17]. We consider a two-dimensional problem in the $(x, z)$ plane, where $x$ is tangent to the soap film at rest and $z$ is the normal axis (figure 7). $z$ is also the transverse displacement of the film, and we call $u$ the tangential liquid velocity inside the film (assumed to be small compared to the transverse velocity). Moreover, the gravity and the inertia of the air are neglected here (they play no role in this mechanism). The equations of motion for the liquid, projected respectively along the transverse axis $z$ and in the plane of the soap film, are:

$$\rho e \frac{\partial^2 z}{\partial t^2} = 2\gamma \frac{\partial^2 z}{\partial x^2} + P\cos(2\pi f t) \tag{6}$$

$$\rho e \frac{\partial u}{\partial t} = F_m + F_c. \tag{7}$$

In equation (6), the first term of the right-hand side describes the interfacial force per unit area that tends to minimize the curvature of the soap film, and $P$ is the amplitude of the acoustic pressure in the tube. To describe the dynamics of the tangential velocity $u$ in equation (7), two forces are in competition, as sketched in figure 7(c). On the one hand, the normal acceleration of the film has a non-zero component in the plane of the soap film, which leads to the inertial centrifugal force per unit area:

$$F_c = -\rho e \frac{\partial^2 z}{\partial t^2} \frac{\partial z}{\partial x}. \tag{8}$$

Assuming $z = A\cos(qx)\cos(\omega t)$, with $q = 2\pi/\lambda_f$ and $\omega = 2\pi f$, the centrifugal force can be written:

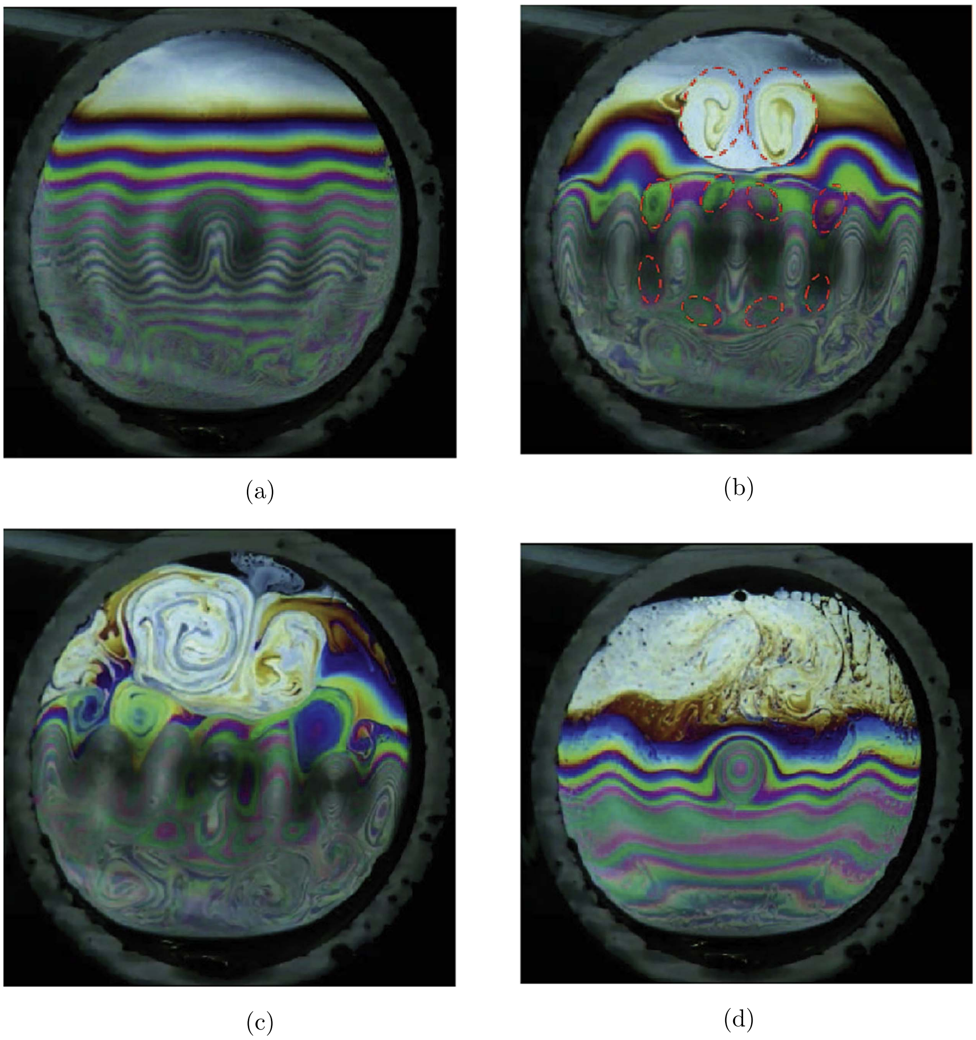


**Figure 8.** Time sequence of the birth and death of vortices. A monochromatic acoustic wave ($f = 450$ Hz, $P = 0.5$ Pa) is set at $t = 0$. (a) $t = 0.1$ s: just after the beginning of the acoustic emission, only self-adaptation is visible. (b) $t = 7$ s: the vortices, that appeared after $t = 1$ s, are growing. For clarity they have been highlighted on the picture by dashed red ellipses: the vortices are organised around the antinodes which are made visible by the tight interference fringes. (c) $t = 12$ s: the vortices grow and accelerate gradually. (d) $t = 17$ s: the vortices disappear although the acoustic excitation is still present.

$$F_{\rm c} = -\rho e\ q\ \omega^2 \frac{A^2}{2} \sin(2qx) \cos^2(\omega t). \tag{9}$$

Since the time-average $\langle \cos^2(\omega t) \rangle = 1/2$ over one period, this force does not average to zero. $F_{\rm c}$ is always directed towards the antinodes: it is thus responsible for the flow of liquid inside the film from the nodes towards the antinodes, leading to the thickening (resp. thinning) of the antinodes (resp. nodes). Hence, a periodic thickness modulation builds up with a spatial period equal to $\lambda_f/2$: $e = e_0 + \delta e \cos(2qx)$. On the other hand, the Marangoni force per unit area:

$$F_{\rm m} = 2\frac{\partial\gamma}{\partial x} = -\frac{E}{e}\frac{\partial e}{\partial x} = +E\frac{\delta e}{e}2q\sin(2qx) \tag{10}$$

tends to homogenize the thickness of the soap film (the elasticity $E$ defined by equation (3) is assumed to be constant).

The existence of a stationary regime implies $\langle F_{\rm c}\rangle = -\langle F_{\rm m}\rangle$, where $\langle F\rangle$ means that the quantity $F$ is time-averaged over a period $1/f$. This leads to $\rho\, e\, \omega^2 q A^2/4 \sim (E/e)\, 2q\, \delta e$. From equation (6) we get $A \sim P/(\rho e\omega^2)$, and we finally obtain:

$$P \sim \omega\sqrt{8\rho\, E\, \delta e}\,. \tag{11}$$

Finally, to compare to our experimental measurements, we assume that the self-adaptation becomes visible when the thickness variation $\delta e$ is of the order of the one corresponding to one fourth of the order of interference (see figure 7(a)): $\delta e_{\rm min} \sim 50$ nm. This leads to a threshold amplitude for the acoustic pressure:

$$P > 2\pi f\sqrt{8\rho E\delta e_{\rm min}} \sim 1.4\times 10^{-3}\ \text{Pa.s}\times f \tag{12}$$

with $E = 0.15$ mN m$^{-1}$ (see section 2.3.2) and $\rho = 10^3$ kg m$^{-3}$. This order of magnitude is in good agreement with our experimental results presented in figure 7(b).

### *3.3. Vortices*

When further increasing the amplitude of the acoustic pressure above the self-adaptation threshold, the system becomes unstable and vortices appear in the soap film. A very rich and complex phenomenology appears. We describe in the photographs of figure 8 a scenario for the appearance and evolution of such vortices, under a continuous monochromatic acoustic forcing suddenly started at $t = 0$. Within a fraction of second, liquid is observed to accumulate around the vibration antinodes and self-adaptation appears as shown in figure 8(a). Then, recirculation of liquid is observed at $t \sim 1$ s and vortices form in the region of thin film around the nodes and in the upper region of thin film of the soap film as shown in figure 8(b). The vortices always appear by a pair of opposite circulation. The vortices then grow and accelerate (figure 8(c)), sometimes merge in pairs, and finally disappear spontaneously after a few seconds (figure 8(d)). After the vortices have disappeared, self-adaptation is still present, and the gradient of thickness is much smaller than in the initial condition of figure 8(a).

The building up of vortices is certainly the key ingredient for the beauty of the experiments, since the liquid is advected whereas the thickness gradients do not disappear: colours are therefore advected as well, producing wonderful dynamical patterns. However, the appearance of vortices invokes complex mechanisms and no simple overall picture exists yet in the literature. In the case of a horizontal soap film vibrated transversally, two main mechanisms have been identified.

Firstly, at sufficiently large acoustic pressure, strong nonlinear effects due to the inertia of the liquid become important, besides Marangoni and centrifugal forces. This non-oscillatory volume forcing, originating inside the liquid, strongly depends on the thickness gradient [16]. In the case of our experiments, the existence of a large thickness gradient due to the gravitational drainage of the film could enhance this non-oscillatory volume forcing of the vortices. Moreover, the spontaneous disappearance of the vortices after a while is concomitant with a decrease in the thickness gradient, which supports this interpretation.

Secondly, another source of non-linearity is due to the motion of the air above and below the film. For high amplitudes in film vibration, inertial effects in the air result in steady

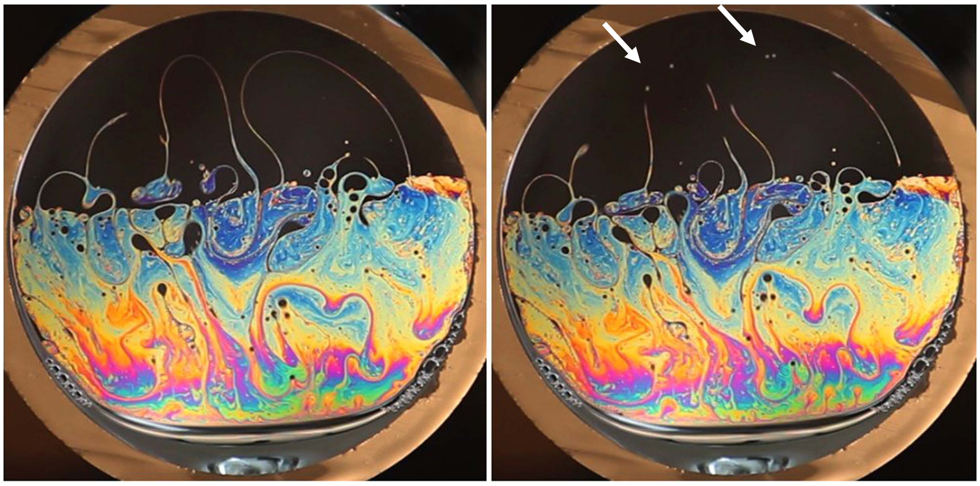

**Figure 9.** 'Bubbles' of black film trapped inside the iridescent film, and drops and filaments of iridescent film inside the black film region. The filaments have been formed during the ascending motion of liquid advected by a vortex before the image is taken. The two images are separated by 0.3 seconds. The rising up of the 2D bubbles is visible, as well as the destabilization of the 2D coloured filaments into 2D droplets, which has been pointed by white arrows. Piece of music: *Lucilla*, from the album 'Aeroplanando', by Choro de Rua (2013).

recirculations with several cellular motions [10, 15, 16] (see [28] about this effect called *acoustic streaming*). This effect is due to the non-linearities of the stress appearing in the Stokes layers and may result in a non negligible tangential flow of the liquid (surface forcing). This flow could lead to a gradient of thickness, and then a gradient of surface tension, reinforcing the competition between opposite forces at the origin of the vortices.

### *3.4. Two-dimensional rising bubbles and falling drops*

The vortices drive zones of inhomogeneous thicknesses, which travel in the soap film and do not merge with the surroundings. The result is spectacular when a significant initial fraction of the soap film surface is a black film, as shown in figures 1 and 9. Two-dimensional (2D) 'bubbles' formed from black film can be trapped inside the iridescent film, and similarly 2D drops of coloured film may be advected in the black film region during the acoustic forcing. These 2D domains behave as if the black film region and the coloured film region were two immiscible phases, separated by a 1D interface. Figure 9 shows that the drops and bubbles are circular, suggesting that the interface tends to be minimal. Moreover coloured filaments fragment into several drops, driven by the interface minimisation. The one-dimensional interface between areas of black film and iridescent film thus behaves like the interface between immiscible phases in 3D system driven by the surface tension: by analogy, a line tension can then be used to describe the line energy of the interface between those 2D domains.

When the acoustic forcing is removed, the bubbles rise up and burst at the 2D surface of the coloured film, mimicking the buoyancy motion of air bubbles in a liquid pool. Why do bubbles rise? As described by equation (2), the hydrostatic pressure inside the vertical soap film at rest equilibrates the gradient of surface tension (the Marangoni force), both depending on the local thickness of the soap film. When a region of black film is trapped inside an

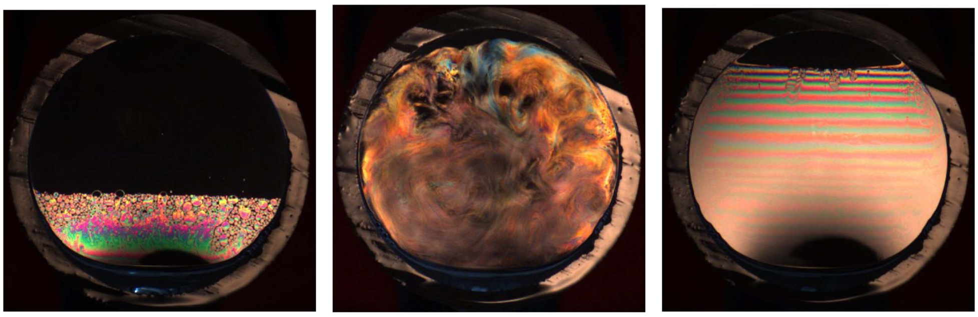

(a) (b) (c)

**Figure 10.** Acoustic swelling of a soap film. (a) In the initial state, a large surface fraction of the vertical soap film is black. (b) The amplitude of the acoustic excitation is suddenly increased: large recirculations of liquid within the whole film is observed. (c) The acoustic forcing is removed: a large surface fraction of the film is now filled with coloured fringes. The time elapsed between each image is $\sim$1 s.

iridescent area of much larger thickness, the local Marangoni force is larger than its weight and the ‘bubble’, experiencing a net upwards force, is driven up until it reaches a region matching its thickness. Everything happens as if the black film drops, even though they have the same density as the surroundings, were lighter and were thus submitted to an Archimedes buoyancy force. Similarly, drops of large thickness which have been dragged into the black film fall down in the iridescent pool until the Marangoni force is large enough to equilibrate their weight.

### *3.5. Swelling the soap film*

Increasing even further the amplitude of the acoustic forcing may result in swelling the soap film previously drained, as illustrated in figure 10. Due to drainage, a large surface fraction of the film is black (figure 10(a)). The acoustic forcing is then set at a high amplitude and a large recirculation of liquid happens as shown in figure 10(b). At the internal bottom of the tube, a liquid pool is always present, coming from liquid dragged during the soap film formation when the end of the tube is dipped in the soap solution, or from the liquid which has drained out of the film. The flow in the plane of the film advects liquid from this reservoir, which swells the soap film. When the acoustic forcing is removed, coloured fringes appear on a large surface fraction of the film in figure 10(c), showing that the film is thicker than initially. This swelling of a vertical soap film using an acoustic wave has to our knowledge never been previously reported in the literature; we plan to investigate this effect in detail in further studies.

## 4. Conclusion: the key of an aesthetic experiment

When the acoustic forcing is the playing of music, all the events described in the previous sections couple, synchronizing the visual events on the music. In this section, we synthesize the phenomena and we show how they combine to produce the impression that we actually ‘see’ what we hear.

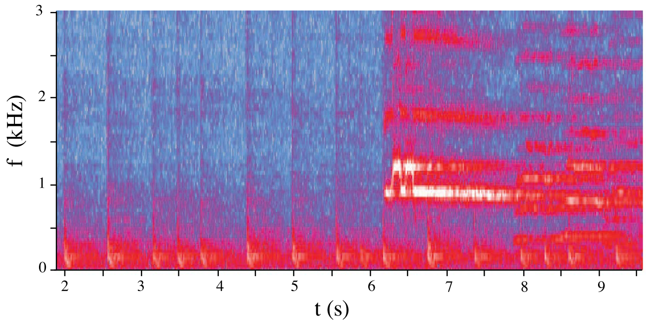

(a)

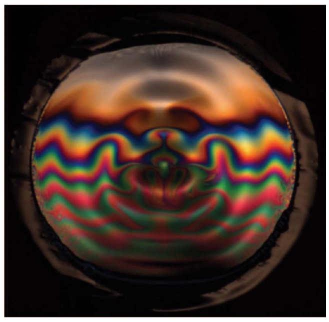
(b)

**Figure 11.** (a) Part of the spectrogram (obtained using the free software Audacity®) from *The Good, the Bad and the Ugly* main theme, soundtrack by Enrico Morricone. The frequency content of the music played is displayed versus time. The corresponding amplitude is indicated by a color code (in arbitrary units): a continuously growing amplitude corresponds to a color successively blue, pink, red and then white. Thus, dominant frequencies appear in white, and reflect the melody of the music play (note that the harmonics, which are multiple frequencies of the fundamental frequency, are also present but at a lower amplitude). A short sequence, having a broad spectrum peaked at 200 Hz, appears regularly in time with a periodicity of $\sim$1 s: this part is played by drums. Between 6 s and 8 s, the principal frequency varies from 900 Hz to 1250 Hz: this part is played by a flute. The second resonant mode of the tube, of length $L = 35.5$ cm, is at 900 Hz (see figure 4). Hence, flow of liquid inside the soap film is observed while the flute is playing, as shown on (b), with a photograph taken at $t = 7$ s. The extract of the piece of music is visible at the following link: https://youtu.be/YC0cZ_xNf-Y.

### 4.1. Choice of tube

The key of the synchronization between music and visualisation resides in the fact that only some frequencies are amplified: the acoustic resonance frequencies of the tube. Phenomena such as self-adaptation, vortices and two-dimensional bubble ejection are more easily obtained at frequencies close to the resonances of the tube, given by equation (1), which depend on the length and on the diameter of the tube. The frequencies of the piece of music can be analyzed using a spectrogram, which represents the frequencies over time, as shown in figure 11: a colour code displays the amplitude of the frequencies. The length and diameter of the tube can thus be adapted for the resonance frequencies of the tube to coincide with the dominant frequencies of the music, which have the highest amplitude. The tube resonance frequencies can also be adapted to the tessitura of the music instrument present in the music. For example, the fundamental frequency of the tube used in our experiments is around 450 Hz (see figure 4), which corresponds to the frequency range covered by a flute, or a soprano voice. As for percussion instruments (drums, piano etc.), their broad acoustic frequency range makes them adapted to excite the resonance frequency of any tube. Hence the acoustically forced patterns on the soap film at the end of the tube synchronize on the rhythm given by the percussion.

### 4.2. The interplay of the characteristic time scales

The generation of vortices is certainly the phenomenon by which liquid is advected in the soap film, producing spectacular effects. In section 3.3, the scenario illustrated in figure 8 is

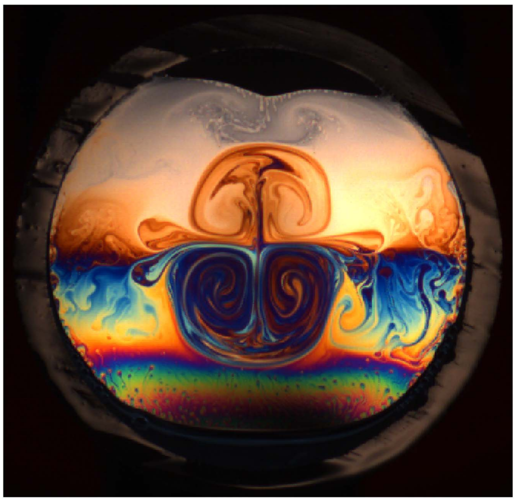

**Figure 12.** A representative example of counter-rotative pairs of vortices obtained with a piece of music, here *The Good, the Bad and the Ugly* main theme soundtrack by Ennio Morricone.

obtained for a continuous monochromatic acoustic excitation, of constant amplitude, emitted during more than 20 s. In the case of a piece of music, the situation is however different. The amplitude is not constant, and both the frequency and the amplitude can vary quickly in time. Vortices can grow and accelerate as previously discussed if the corresponding frequency is played at a large enough amplitude within a few seconds. The photograph in figure 12 is a representative example of counter-rotative pairs of vortices observed using music as an acoustic forcing. However the characteristic time for their spontaneous disappearance described in figure 8 is never reached. With a piece of music vortices disappear rather due to a change of frequency and/or amplitude.

More generally, the observed dynamical patterns involve many characteristic times: one characteristic time for the gravity-induced drainage of liquid in the film ($\sim$10 s), another for the self-adaptation phenomena ($\sim$0.1 s), for the development of vortices ($\sim$1 s), and for their disappearance under forcing ($\sim$10 s), which reveal the richness of the physics behind those dynamical patterns. Moreover, some characteristic times are also associated to the advection of iridescent domains within the black film. All those characteristic times are involved in the dynamical response of the soap film to the acoustic forcing produced by a music play: they play a major role in the aesthetics of the experiment.

### *4.3. Increasing the life-time of the soap film*

Due to the drainage, the soap film gets thinner over time, and thus more fragile, i.e. more likely to burst. To avoid the soap film bursting over several minutes, the film can be swollen by increasing the amplitude of the acoustic forcing, as shown in figure 10. Furthermore, this mechanism brings the iridescent soap film into the field of view, and new coloured patterns can be formed. However, one must be careful in increasing the forcing amplitude, since a very large amplitude could lead to the soap film bursting [29].

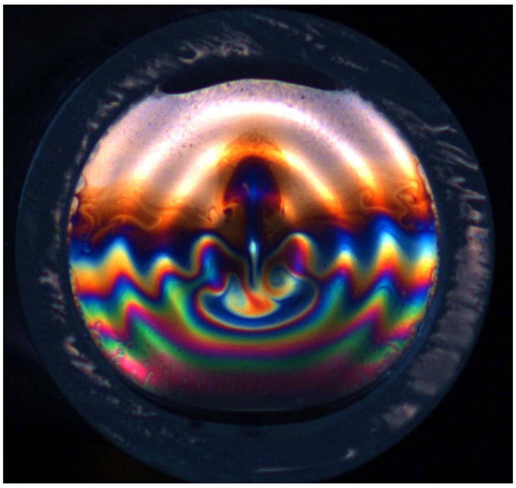

**Figure 13.** Photograph of a soap film presenting at the same time: capillary waves, self-adaptation and the beginning of vortices. Piece of music: *The Lonely Shepherd*, from the album 'Kill Bill Vol. 1 Original Soundtrack', by Gheorghe Zamfir.

### *4.4. To conclude*

We emphasize on the fact that, even if each phenomenon can be described separately, they generally occur simultaneously. In figure 13 for instance, we can see the concentric bright rings of capillary waves, the deformation of the coloured fringes due to self-adaptation, and also the beginning of vortices at the centre of the film.

To conclude, we have shown the rich and complex dynamics of a soap film in response to a non-continuous sound wave. These physical phenomena involved tackling acoustics, optics and hydrodynamics. Hence, this experiment is a good candidate for teaching physics in a classroom or for science popularization. Furthermore, the spectacular effect produced by the synchronization of the video and the music makes of this experiment an interesting tool for art and science projects. Finally, this work has also opened a still unexplored research trail based on the acoustic swelling of the soap film.

## Acknowledgments

We warmly thank our colleagues F Graner, L Rose, and V Leroy for the fruitful and enthusiastic discussions. This work was supported by the French Agence Nationale de la Recherche (ANR) through the project SAMOUSSE (ANR-11-BS09-001).

## References

[1] Aristotle 1984 Sense and sensibilia *Complete Work of Aristotle, Vol 1: The Revised Oxford Translation* (Princeton, NJ: Princeton University Press)
[2] Newton I 1704 *Opticks, or a Treatise of the Reflexions, Refractions, Inflexions and Colours of Light* (London: William Innys)
[3] Rimington A W 1912 *Colour-Music: The Art of Mobile Colour* (London: Hutchinson)
[4] The National Gallery 2015 Soundscapes: retrieved 28 November 2016 from https://nationalgallery.org.uk/whats-on/soundscapes

[5] Stanford N 2014 CYMATICS: Science Vs. Music: retrieved 4 January 2017 from https://vimeo.com/111593305
[6] Boys C V 1890 *Soap Bubbles and the Forces which Mould Them* (London: SPCK)
Boys C V 1959 *Soap Bubbles, their Colours and the Forces which Mould Them* (New York: Dover)
[7] Rämme G 1998 *Soap Bubbles in Art and Education* (Singapore: Science Culture Technology Publishing)
Rämme G 2006 *Experiments with Soap Bubbles and Soap Films* (Uppsala: Kopieringshörnan ABC)
[8] Lovett D R 1994 *Demonstrating Science With Soap Films* (Bristol: Institute of Physics Publishing)
[9] Isenberg C 1987 *The Science of Soap Films and Soap Bubbles* (Clevedon: Tieto)
reprinted Isenberg C 1992 (New York: Dover)
[10] Couder Y, Chomaz J-M and Rabaud M 1989 *Phys.* D **37** 384
[11] Seychelles F, Amarouchene Y, Bessafi M and Kellay H 2008 *Phys. Rev. Lett.* **100** 144501
[12] Tylor E B 1877 *Nature* **16** 12
[13] Taylor S 1878 *Proc. R. Soc.* **27** 71
[14] Joosten J G H 1984 *J. Chem. Phys.* **80** 2383
[15] Afenchenko V O, Ezersky A B, Kiyashko S V, Rabinovich M I and Weidman P D 1998 *Phys. Fluids* **10** 390
[16] Vega J M, Higuera F J and Weidman P D 1998 *J. Fluid Mech.* **372** 213–30
[17] Boudaoud A, Couder Y and Ben Amar M 1999 *Phys. Rev. Lett.* **82** 3847
[18] Kosgodagan Acharige S, Elias F and Derec C 2014 *Soft Matter* **10** 8341
[19] Elias F, Hutzler S and Ferreira M S 2007 *Eur. J. Phys.* **28** 755
[20] Rossing T D 2007 *Handbook of Acoustics* (New York: Springer)
[21] Ogawa N and Kaneko F 2013 *Eur. J. Phys.* **34** 1159–65
[22] Delly J G 2003 The Michel-Lévy interference color chart microscopy's magical color key https://mccrone.com/mm/the-michel-levy-interference-color-chart-microscopys-magical-color-key/
[23] Cantat I, Cohen-Addad S, Elias F, Graner F, Hohler R, Pitois O, Rouyer F and Saint-Jalmes A 2010 *Les mousses, Structure et Dynamique* (Paris: Belin)
Cantat I, Cohen-Addad S, Elias F, Graner F, Hohler R, Pitois O, Rouyer F and Saint-Jalmes A 2013 *Foams: Structure and Dynamics* ed S J Cox (Oxford: Oxford University Press) (Engl. transl.)
[24] Schwartz L W and Roy R V 1999 *J. Colloid Interface Sci.* **218** 309
[25] Champougny L, Roché M, Drenckhan W and Rio E 2016 *Soft Matter* **12** 5276
[26] Elias F, Bacri J-C, Flament C, Janiaud E, Talbot D, Drenckhan W, Hutzler S and Weaire D 2005 *Colloids Surf.* A **263** 65
[27] Elias F, Kosgodagan Acharige S, Rose L, Gay C, Leroy V and Derec C 2017 *Colloids Surf.* A in press (https://doi.org/10.1016/j.colsurfa.2017.02.091)
[28] Nyborg W L 1958 *J. Acoust. Soc. Am.* **30** 329
Lighthill J 1978 *J. Sound Vibr.* **61** 418
[29] Drenckhan W, Dollet B, Hutzler S and Elias F 2008 *Phil. Mag. Lett.* **88** 1669